Optica Applicata, Vol. XXIII, No. 2–3, 1993

Theoretical model of TEA nitrogen laser excited by electric discharge
Part 2. Results of calculations

J. MAKUCHOWSKI, L. POKORA

Laser Technics Center, ul. Kasprzaka 29/31, 01–234 Warszawa, Poland.

The results of calculations of characteristics of atmospheric nitrogen laser of TEA type were obtained by applying the formerly elaborated theoretical model described in Part 1 of this work [1]. The results reported show the influence of particular design and external parameters of the laser on its characteristics. The presented results of calculations are qualitatively and quantitatively consistent with the results published in the papers mentioned in this paper [3]–[6], [8], [9].

1. Description of the numerical programme

Theoretical model of nitrogen laser described in the first part of this paper has been presented schematically in a block diagram in Fig. 1. The numerical programme realizing this theoretical model has been written in Fortran language. The block scheme of this computer programme is shown in Fig. 2.

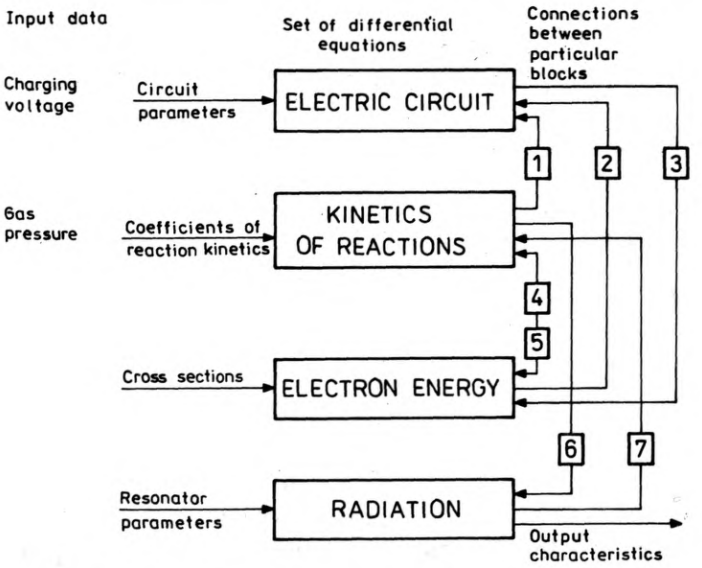

Fig. 1. Block scheme presenting the constructed theoretical model of nitrogen laser. 1 – electron density, 2 – electron mobility, 3 – electric field strength, 4 – coefficients of reaction kinetics, 5 – population of levels, 6 – photon density, 7 – population of laser levels

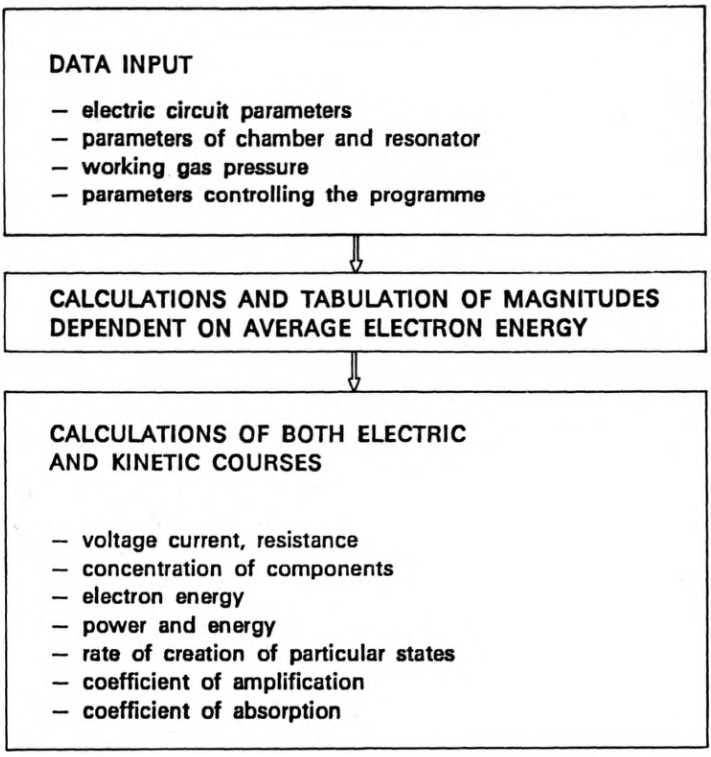

Fig. 2. Block scheme of numerical operation of programme for calculation of nitrogen laser

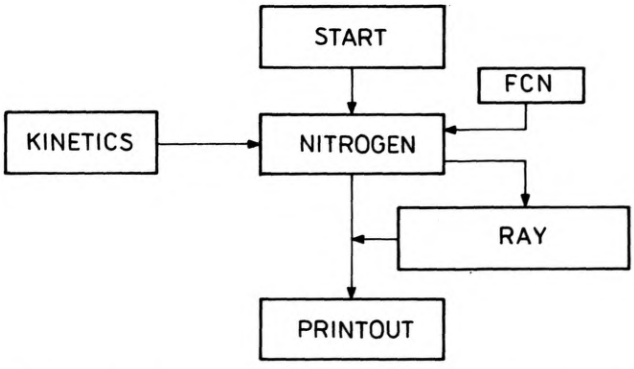

Fig. 3. Block scheme presenting the construction of the numerical programme to calculate the nitrogen laser

The programme consists of several subroutines which have been presented schematically in Fig. 3. Their short characteristics are described below.

– START: programme preparing the data concerning the processes taking place in the medium. These are: rate coefficients, in the case of the cross-section for electron collisions with atoms or molecules as a function of electron energy and the corresponding energy differences in the case when those collision happen. For the

latter case the programme performs an integration of the cross-section with a given electron distribution function. Some of data exploited in this programme are contained in the Table.

– NITROGEN: main programme, which reads the basic data about the laser parameters and controls the whole of the programme.

– KINETICS: subroutine reading the information about the working factor. It computes the electron mobility as a function of energy as well as the rate of energy loss due to elastic collisions.

– FCN: subroutine solving the set of equations basing on the Gear algorithm for the method of backward differentiating. It takes advantage of the library procedure DGEAR (elaborated in IMSL).

– RAY: subroutine receiving the corresponding results from the main programme. It solves the equation for radiation intensity.

– PRINTOUT: subroutine ordering the results in a needed form adjusted to printout and drawing the figures with the help of either a printer or a plotter.

This programme has been tested to be selfconsistent. The tests were performed for the following set of data.

Electric parameters

– capacities: $C_L = C_R = 6.3$ nF,
– inductances: $L_I = 16$ nH, L_2, $L_3 = 1$ nH,
– supply voltage: 20 kV.

Geometric and optical parameters

– effective sizes of chamber (discharging volume): $l_G = 48$ cm, $D_{ch} = 0.375$ cm, $S_{ch} = 0.1$ cm,
– length of the resonator: $L_r = 48$ cm,
– distance between the preionization electrodes: $d_p = 0.6$ cm,
– reflection coefficients of the mirrors (for $\lambda = 337.1$ nm): $R_1 = 0.1$, $R_2 = 0.99$.

Gas pressure in the laser chamber

– $p = 1013$ hPa.

The numerical correctness of the programme was estimated on the basis of three criteria:

1. Consistence of the balance of energy accumulated in capacitors and liberated in elements of the electric circuit.
2. Consistence of the electron energy balance.
3. Consistence of the electric charge balance.

The value of energy accumulated in the battery of capacitors C_L and C_R amounted to $E_0 = 2.52$ J for the time $t = 0$. The sum of energy accumulated and liberated in particular elements of the circuit elements was calculated by the programme at each time step. This sum was contained within the limits from 2.5 J to 2.54 J. This gives the relative error $<0.8\%$.

The other two criteria were satisfied with an error of $+0.1\%$. Such a dependence was maintained for each moment of time. Very good consistence of all three balances substantiates the correctness of the numerical programme.

The above programme has been installed in a 286 IBM AT microcomputer of 8 MHz clock. The set of equations describing the processes taking place during the electric discharge in the nitrogen laser chamber is characterized by great differences between the moduli of eigenvalues. Thus, it is a set of poor-contained (stiff type) equations [2]. Its solution requires a suitable numerical method. The most commonly applied methods are those of Hamming, R-K-Treanor, Adams, R-K-Gill. During realization of this programme we took advantage of the Gear procedure which is especially useful to solve the set of stiff class equations being easily available at the same time.

All the results presented in the further parts of this paper were achieved on IBM PC AT microcomputers equipped with coprocessor. The coupling time for one full run was on average as high as 3 hours of the processor work.

During calculations the data-set DATA 1 was used. The rate coefficient for reactions tabulated as functions of electron temperatures are there collected. The programme is written in the way enabling the laser characteristics to be received as functions of each of parameters used to description. The values of these parameters were changed in a broad range.

2. Results of calculations of nitrogen laser characteristics

In the first phase of calculations, a number of numerical programme tests were made. A preliminary analysis of the influence of particular collision reactions on the laser medium kinetics has been carried out. This analysis consisted in defining what percentage is introduced in a given moment of time by the analysed reaction to the concentration of the given kind of particle. In this way, the reactions of numbers 68–70, 72–74 from Tab. 1 (Part 1 of this paper [1]) were eliminated. Their contribution to concentration of the given kind of particle did not exceed 0.1%. These all appeared to be reactions of different type of recombinations which were much slower than the others. This resulted in restriction of the number of reactions encountered in the model to 68.

Table. List of parameters of nitrogen laser accepted for calculations

Electric parameters
- capacities: $C_L = 6.3$ nF, $C_R = 6.3$ nF,
- supplying voltage: $U_0 = 20$ kV,
- inductancies: $L_1 = 16$ nH, $L_{2,3} = 1$ nH.

Geometric and optical parameters
- effective sizes of the chamber*: $L \times W \times H = 48 \times 0.1 \times 0.375$ cm,
- resonator length: $L_r = 48$ cm,
- reflection coefficients of the mirror: $R_1 \approx 99\%$, $R_2 \approx$ %.

Gas parameters
- technical nitrogen at the pressure: $p = 1013$ hPa,
- free flow of gas.

* Discharging chamber of the laser is understood as a interelectrode space in which electric discharge occurs.

The laser characteristics presented in this paper have been obtained for the initial conditions and input parameters presented in the Table. In most cases, these are typical values of nitrogen lasers. A part of those has been imposed by the accepted requirements with respect to the laser design and the available condensers accumulating the electric energy. Taking advantage of the model described the calculations for the laser (of TEA type) operating at the atmospheric pressure were performed.

2.1. Electric processes

The results of calculations of electric runs of both voltage and current in the electric circuit of the laser are shown in Fig. 4. The time $t = 0$ corresponds to the moment of short-circuit in the commutator. The commutator starts rapidly to conduct the current. After 2 ns the voltage drops from its initial value of 21 kV to the value below 8 kV, while its resistance achieves the value of about 2 Ω during this time. In the moment of electric breakdown in the chamber and appearence of an electric current pulse, the commutator is in the state of full conductance of the current ($R_I \approx 0.03$ Ω) [3]. The voltage at the main electrodes increases up to the value of 32 kV during 28 ns, which makes the average rate of increase to be equal to about 1.1×10^{12} V/s. After the breakdown in the laser chamber the voltage on the electrodes begins to drop, while the current intensity increases rapidly in the chamber. It reaches the value of 18 kA in the time of 3 ns which gives the average rate of current increase at the level of 6×10^{12} A/s [4]. During the current pulse the quasi-equilibrium conditions are being established in the plasma of the laser medium. This equilibrium occurs for lowered electron energy as compared to the avalanche stage. This is presented in Fig. 5, where the time-varying chamber resistance and the average electron temperature are shown with the voltage and current pulses taken as the background. Both qualitatively and quantitatively the

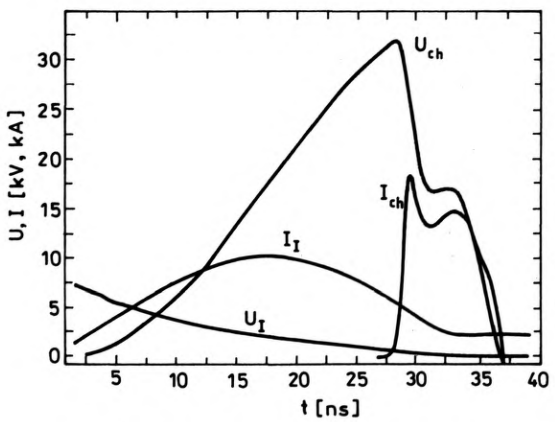

Fig. 4. Variation of voltage (U) and current (I) in the electric circuit of the laser (indices denote: I — commutator, ch — chamber)

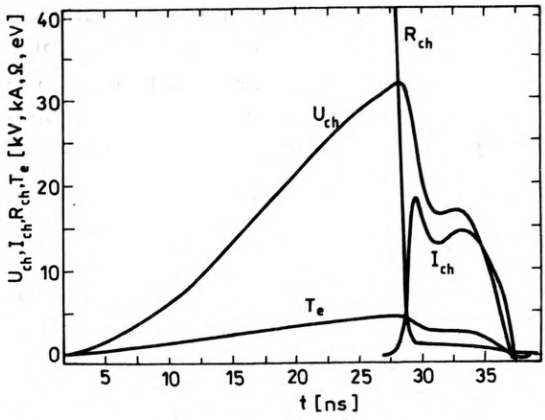

Fig. 5. Time change of both the electric resistance R_{ch} in the chamber and the electron energy T_e with current I_{ch} and voltage V_{ch} pulses taken as the background

run of interelectrode voltage and electron energy are consistent with the results of paper [5]. The minimal electric resistance of the chamber amounts to about 0.15 Ω. For the sake of comparison, let us notice that in paper [6] the measured electric resistance of the chamber was equal to about 0.1 Ω.

For practical reasons, it is essential to find the connection between design and exploitation parameters and the parameters of laser radiation. This problem is the subject of consideration in the next sections of this paper.

2.2. Time evolution of N_2 active medium

Active medium of the nitrogen laser contains a great number of particles of different kinds (atoms, molecules in the excited state or ionized), which have a direct or indirect influence on the N_2 concentration in the upper and lower laser states. In

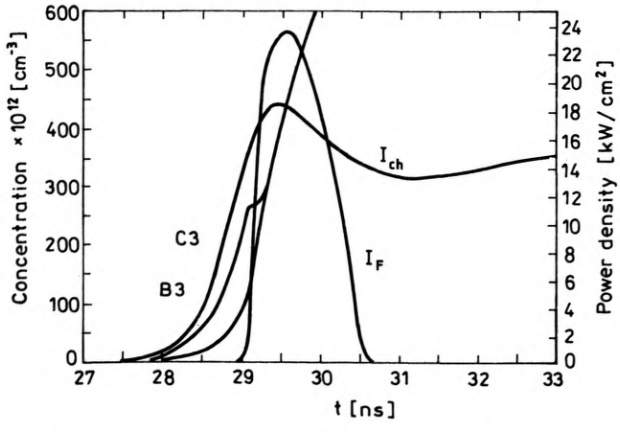

Fig. 6. Evolution concentration: $N_2(C^3\Pi_u, v = 0)$ — upper laser level C3, $N_2(B^3\Pi_g, v = 0)$ — lower laser level B3, of the discharge current I_{ch} of the chamber and the radiation power density I_F

Figure 6, the time evolution of populations of the upper and lower laser levels, the discharge current of the chamber and the emitted radiation power density have been presented. During the time evolution of $N_2(C^3\Pi_u)$ concentration a distinct maximum is observed. It amounts to about 4×10^{14} cm^{-3}. On the other hand, the concentration of $N_2(B^3\Pi_g)$ states increases all the time while the pumping discharge lasts (the state B is metastable). The laser action developes very quickly and is connected with an avalanche increase of photon concentration. Generation of laser radiation pulse causes the total decay of the population inversion. This is a characteristic feature of nitrogen lasers working in the superradiation regime.

3. Laser characteristics as a function of design parameters

In this section, the influence of electric circuit capacity and the interelectrode distance on the current-voltage characteristics, radiation and efficiency has been shown. The efficiencies used in this work, *i.e.*, internal η_i, electrical η_E and total η_t, are defined as follows:

$$\eta_i = \frac{E_L}{E_R}; \quad \eta_E = \frac{E_R}{E_w}; \quad \eta_t = \eta_i \eta_E$$

where: E_L – energy of the laser radiation pulse,
E_R – electric energy liberated in the laser chamber during the laser pulse,
E_w – energy accumulated in capacitors C_R and C_L at $t = 0$.

3.1. Capacity influence

The influence of capacity on the laser parameters has been analysed by changing the capacity C_L. The calculations were carried out for the values: $C_L = C_R = 4, 5, 6.3, 8, 9, 12.6$ nF. The basis for the assumption of such a construction of the system of energy accumulation ($C_L = C_R$) were the considerations given in paper [7]. These

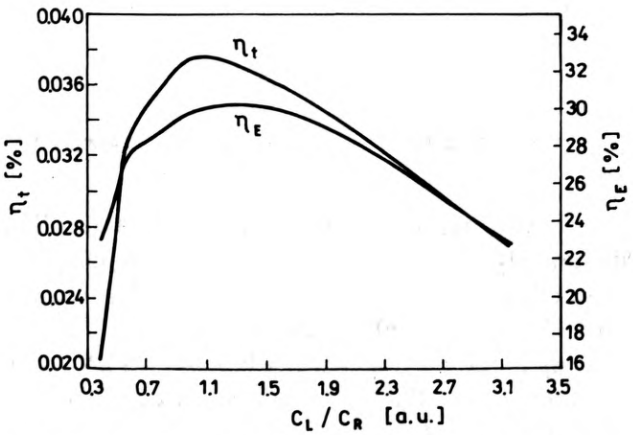

Fig. 7. Total η_t and electric η_E efficiency of nitrogen laser as functions of capacity ratio C_L/C_R

were confirmed by the results of our own calculations presented in Fig. 7. Maximal total and electric efficiencies, described by the formulae below, are achieved when the capacity ratio $C_L/C_R \approx 1-1.2$. The remaining laser parameters were such as those in the table.

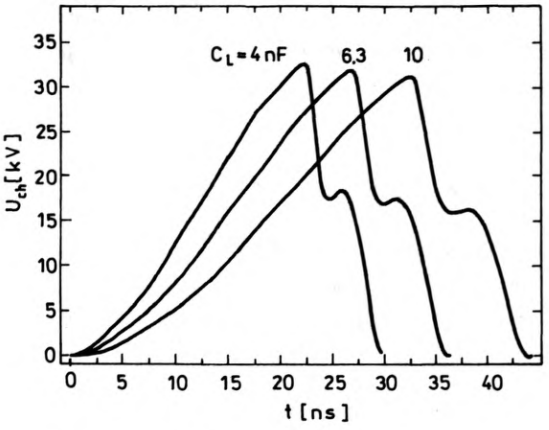

Fig. 8. Variation of the electric voltage U_{ch} in the laser chamber parametrized with respect to the chosen capacities C_L

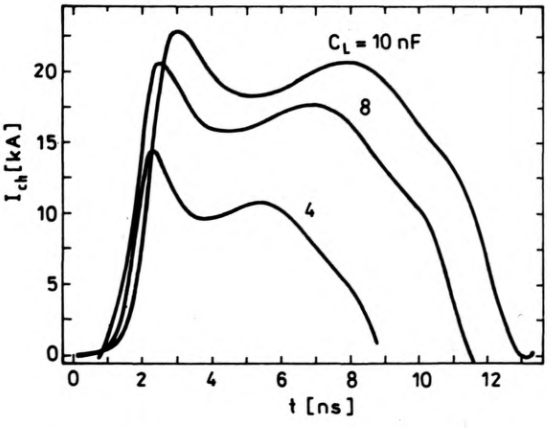

Fig. 9. Variation of the electric current I_{ch} in the laser chamber for different capacities C_L. The beginnings of the pulses have been shifted to the point $t = 0$

The runs of voltages and currents in the chamber are shown in Figs. 8 and 9. The shape of the voltage pulse is qualitatively consistent with the results reported in paper [8]. Together with the increase of capacity C_L the value of maximal voltage in the chamber diminishes (from about 32.5 kV for 4 nF to about 30.55 kV for 10 nF) which is connected with slower charging of the greater capacity (about 1.48 kV/ns for $C_L = 4$ nF to about 0.95 kV/ns for $C_L = 10$ nF). The maximal value of current intensity in the chamber increases from about 14 kA for $C_L = 4$ nF to about 23 kA for $C_L = 10$ nF. The value of the condenser capacity C_L has an essential influence

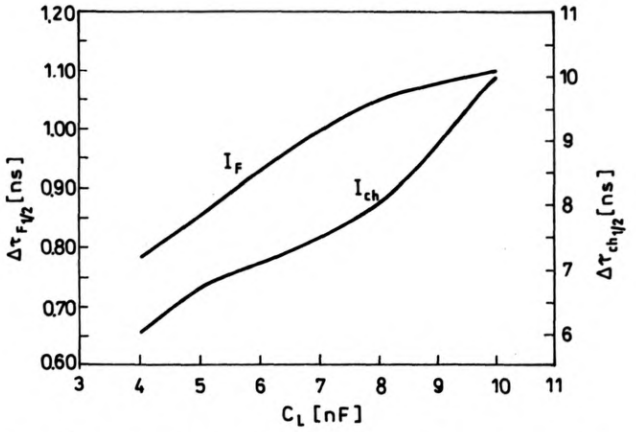

Fig. 10. Duration of the electric pulse I_{ch} and the pulse of the laser radiation I_F as a function of capacity C_L

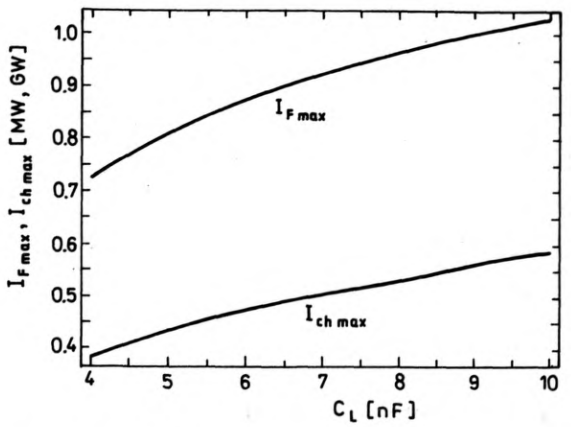

Fig. 11. Peak power of laser radiation $I_{F max}$ and electric power $I_{ch max}$ produced in the discharge chamber as a function of the capacity C_L

on duration of both electric pulse and radiation. This dependence is shown in Fig. 10. For small capacities these times are short (for instance, for $C_L = 4$ nF the halfwidth time of electric pulse duration amounts to $\Delta\tau_{1/2} \approx 6$ ns and for radiation — about 0.8 ns) and increases together with the increase of capacity (on average by 30–40%).

This halfwidth time of the pulse was calculated using two methods — as a time difference, for which the power is equal to the half of the maximal power, and as a product of pulse energy and maximal power. In both the cases the values obtained showed high consistence (relative error $< 2\%$). In this work, the results of measurements obtained by means of the first method are presented. The highest values of the electric power liberated in the chamber as well as those for radiation shown in Fig. 11 are achieved for $C_L = 10$ nF (for about 0.59 GW and above 1 MW,

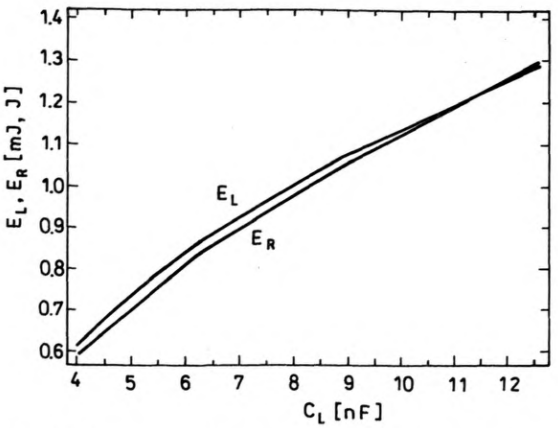

Fig. 12. Laser radiation energy E_L and electric energy E_R liberated in the chamber during the time of the radiation pulse generation as a function of capacity C_L

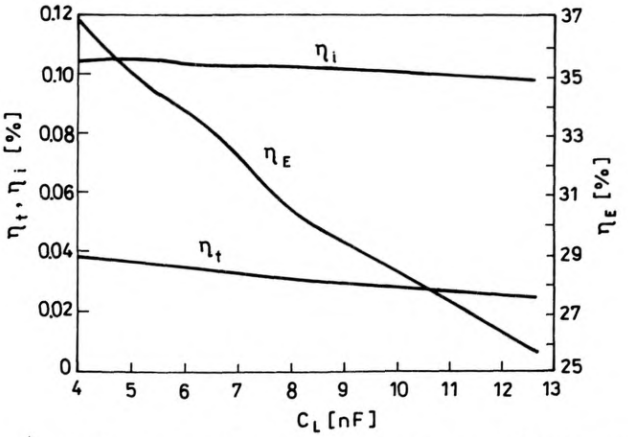

Fig. 13. Total η_t, internal η_i and electrical η_E efficiencies each as a function of capacity C_L

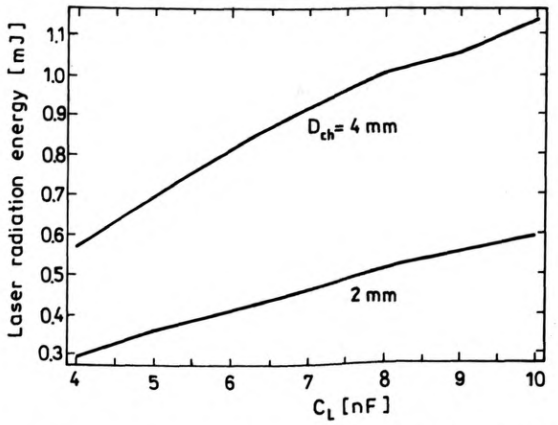

Fig. 14. Laser radiation energy as a function of capacity C_L for different distances of electrodes in the laser chamber (D_{ch} and $2D_{ch}$)

respectively). The value of energy liberated in the chamber and that of energy radiated out increase with the increase of capacity. Their highest values within the examined range of capacity changes were about 1.303 J and 1.29 mJ for $C_L =$ 12.6 nF which may be seen in Fig. 12. The presented values of electric energy liberated in the chamber concern only the time period till the end moment of the laser radiation pulse. This is the energy a part of which has been transferred into laser energy. Obviously, after pulse generation the discharge lasts further without causing any inversion in the medium (Fig. 6). This part of energy is, thus, totally lost causing an increase of molecule concentration in metastable state and an increase of the active medium temperature. This is a harmful phenomenon from the point of view of laser generation but if the medium flows through the region of discharge no influence on the next pulse extraction is evoked.

In Figure 13, the laser efficiency is presented. Maximal values of efficiency outside the internal efficiency cannot be achieved in the examined range of variability of capacity. The highest values of efficiency η_t amount, respectively, to about 0.038% (for $C_L = 4$ nF), while η_i (maximal value) is equal to about 0.105% (for $C_L = 5$ nF). The character of these dependences corresponds accurately to the dependence of energies radiated and liberated in the chamber on the condenser capacity C_L. In Figure 14, the calculated dependence of radiation energy on the capacity C_L for two distances of electrodes D_{ch} and $2D_{ch}$ in the laser chamber is presented. For greater D_{ch} (less E/N) the dependence is sharper.

3.2. Influence of the interelectrode distance

Evaluation of the influence of the electrode distance in the chamber on the output parameters of N_2 laser has been done for $D_{ch} = 3.3-4.2$ mm. The other parameters of the laser are shown in the Table. The runs of voltages and currents are presented in Figs. 15 and 16. The values of the maximal voltage on the electrodes of the chamber increase with the increase of the electrode distance (from 27 kV for

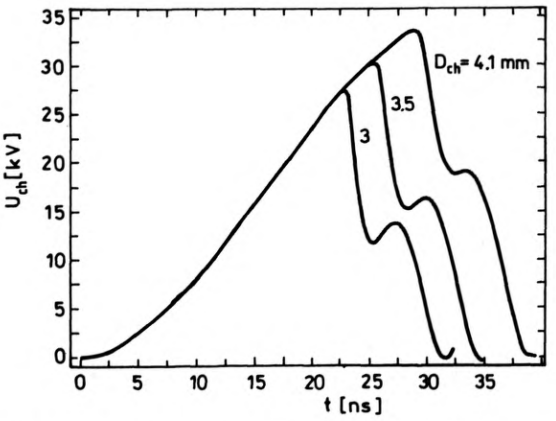

Fig. 15. Run of the voltage U_{ch} in the laser chamber parametrized with respect to the distance between the electrodes D_{ch}

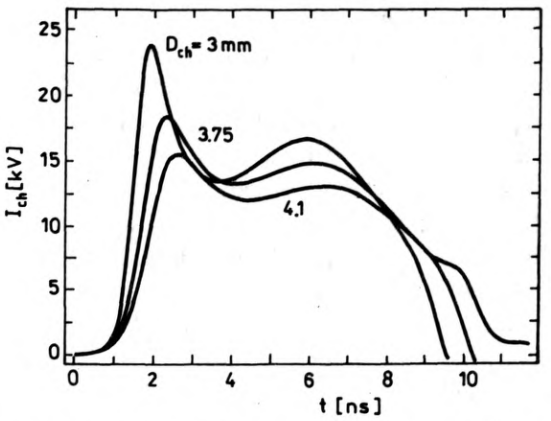

Fig. 16. Variation of the current I_{ch} in the chamber parametrized with respect to the distance between the electrodes D_{ch}

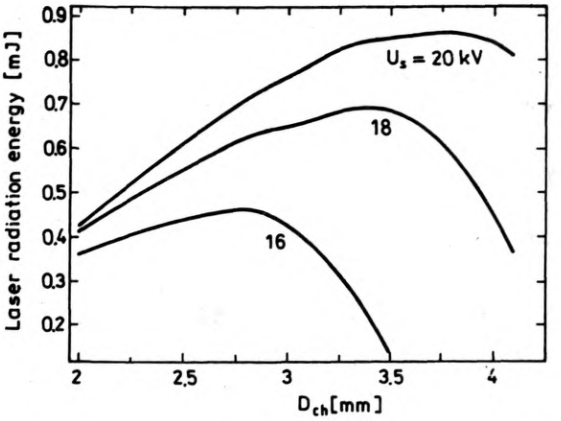

Fig. 17. Output energy of the laser radiation as a function of interelectrode distance parametrized with respect to the supply voltage U_s

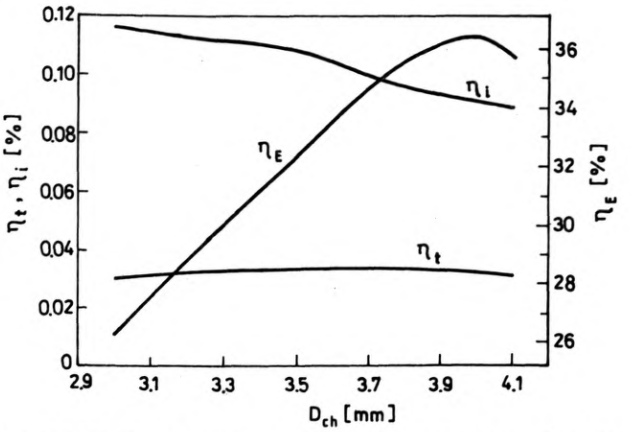

Fig. 18. Total η_t, internal η_i and electric η_E efficiences of the laser as functions of interelectrode distance

$D = 3$ mm to 34 kV for $D = 4.1$ mm). This is an almost linear increase. The maximal value of the chamber current intensity increases with the decrease of interelectrode distance from 15 kV for $D_{ch} = 4.1$ mm up to 24 kA for $D_{ch} = 3$ mm. On the other hand, the current pulse width as well as the halfwidth time of the laser radiation pulse duration are almost independent of D_{ch}. Maxima of the total and electric efficiencies amount to about 0.034% (for $D_{ch} = 3.75$ mm) and about 36.4% (for $D_{ch} = 4$ mm), respectively.

In Figure 17, the influence of the interelectrode distance for established supplying voltage on the output radiation energy is presented. For each supply voltage an optimal interelectrode distance may be found. Thus, for $U_s = 15$ kV, $D_{opt} = 28$ mm and and for $U_s = 20$ kV, $D_{opt} = 3.8$ mm. Together with the increase of the voltage supplying the laser head the value of the optimal distance is shifted toward the higher values.

As it is shown in Figure 18, the internal efficiency diminishes together with the increase of interelectrode distance and changes from about 0.12% ($D_{ch} = 3$ mm) to about 0.095% ($D_{ch} = 4.1$ mm).

3.3. Influence of the length of the discharging electrodes

The influence of the discharge electrode length of a nitrogen laser on the output energy of the laser radiation has been estimated. In the case discussed, the resonator consisting of a mirror of $R \approx 100\%$ and a plano-parallel plate of reflection coefficient $\approx 10\%$ has the length equal to the length of the electrode. It has been assumed that the electrodes were positioned paralelly with respect to each other. The results of simulation are presented in Fig. 19. Optimal electrode length amounts to about 50 cm. Its increment above this value results in an inessential increase of pulse energy, for instance, $\Delta L = 20$ cm (which corresponds to electrodes longer by 40%) causes $\Delta E_L = 0.025$ arbitrary units (thus, the radiation energy pulse is higher by about 1.5%).

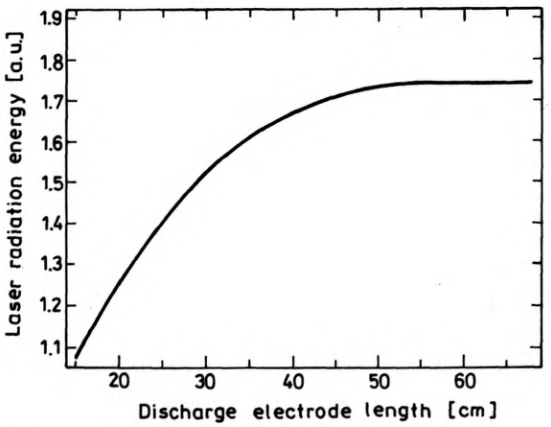

Fig. 19. Laser radiation energy (arbitrary units) as a function of the discharge electrode length

4. Influence of the supply voltage

The typical runs of voltage and current intensity for different supply voltages of capacitors are presented in Figs. 20 and 21. Maximal value of voltage on the chamber electrodes depends weakly on the supply voltage U_s and changes within the limits of 25–32 kV. Similar dependence was reported in paper [9]. Dependence of the maximal current flowing in the chamber on the supply voltage U_s, which changes within the limits of 4–21 kA, is much stronger. For the voltages lower than 10 kV no breakdown occurs in the gas, while the radiation pulse appears first for the voltages above 15 kV. The electric energy liberated in the chamber (during the time of radiation pulse generation) and the radiation energy

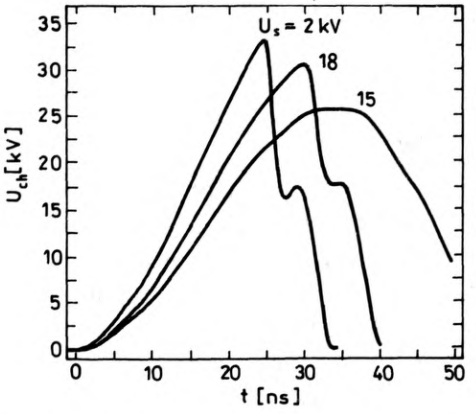

Fig. 20. Variation of the electric voltage U_{ch} in the chamber for different supply voltages U_s. The beginning of each pulse being located in $t = 0$

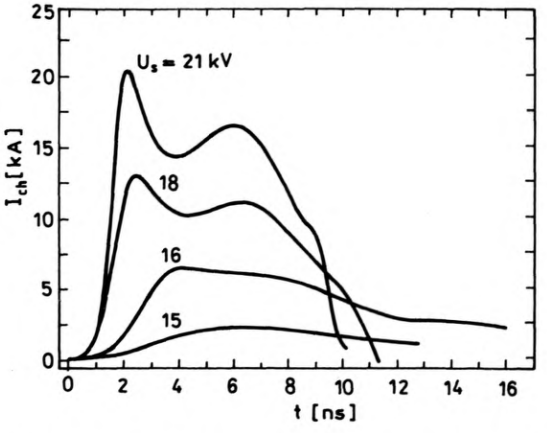

Fig. 21. Variation of the electric current I_{ch} in the chamber for different supply voltages U_s. The beginning of each pulse was located in $t = 0$

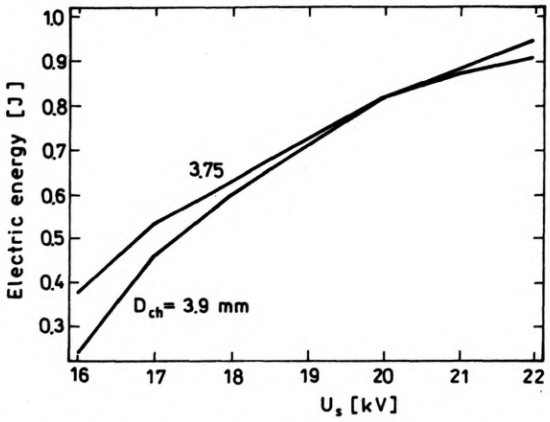

Fig. 22. Electric energy E_R liberated in the chamber till the end moment of the laser pulse generation as a function of supplying voltage

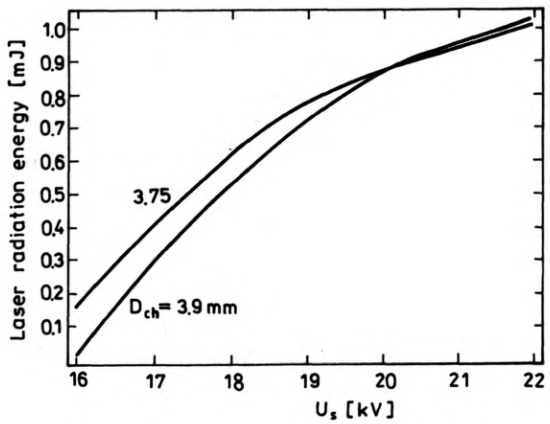

Fig. 23. Radiation energy as a function of the supplying voltage parametrized with respect to the interelectrode distance

are presented in Figs. 22 and 23. The values of both energies increase relatively quickly with the increase of the supplying voltage U_s to the value of about 19.5 kV; these increments, however, become less for the supply voltage higher than 20 kV. Qualitatively it is consistent with the results of calculations presented in [5]. The energy liberated in the chamber changes from 0.25 J to 1 J for the change of U_s from 16 kV to 22 kV. The radiation energy changes respectively from 0 to almost 1.1 J. Maximal powers change similarly.

The total, internal and electric efficiencies as functions of supply voltage were presented in Fig. 24. The efficiencies η_t and η_E reach their maximal values for the voltage equal to about 20.5 kV. They amount respectively to: 0.034% and 32.46%. On the other hand, the efficiency η_i reaches the maximal value 0.111% for the maximal applied voltage 22 kV.

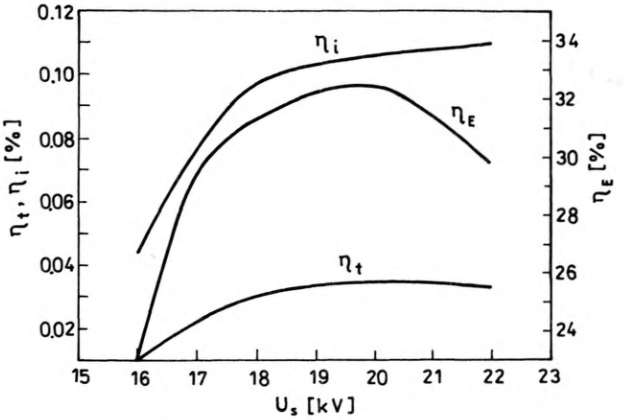

Fig. 24. Laser efficiencies (η_t, η_E, η_i) as functions of the supply voltages

5. Summary

The complete quantitative characteristics of N_2 laser for concrete experimental conditions was obtained. Besides, the results illustrating the influence of the particular design and external parameters on the due characteristics were reported. The model presented described correctly the characteristics of the underpressure (TE) and atmospheric (TEA) lasers. The results of calculations for the TEA type lasers presented above remain in good consistence, both qualitatively and quantitatively with the results reported in the papers mentioned in this work. The experimental verification of some of the obtained results of calculations, for instance, the current-voltage characteristics or the time-evolution of concentration of particular components of the laser plasma, is extremely difficult and sometimes even impossible. Nevertheless, their cognitive value for recognizing the phenomena taking place during discharge in the nitrogen laser medium is esential. The model constructed was used to work out the project brief foredesign accepted to build the nitrogen lasers of both (TE and TAE) types. The paper presents the most important problems connected with numerical modelling of the nitrogen laser operation. The topic being wide and complex is far from being exhausted. In this paper, the analysis of nitrogen laser has been reduced to determination of four output parameters – pulse energy, top power, pulse length and efficiency.

References

[1] MAKUCHOWSKI J., POKORA L., Opt. Appl. **23** (1993), 113,

[2] KRUPOWICZ A., *Metody numeryczne zagadnień początkowych równań różniczkowych zwyczajnych* (in Polish), [Ed.] PWN, Warszawa 1986.

[3] GRATTON R., MANGIONI S., NIEDBALSKI J., VALENT R., Phys. E: Sci Instrum. **21** (1988), 851.

[4] GRIGORYAN YU. L., PAPANYAN V. O., *Issledovanie elektrorazryadnogo azotnogo lazera bliskogo davleniya*, Preprint IYUI–78–80, Erevan 1978.

[5] DZAKOWIC G., KAN T., KUENNING R., SCHLIFT L., *Design study of high average power* (20–100 watts) *pulsed nitrogen lasers at* $\lambda = 3371$ Å, Lawrence Livermore Laboratory Report UCID–16733, 1975.

[6] SMITH A. J., KWEK R. H., TOU T. Y., GHOLAP A. V., LEE S., IEEE J. Quantum Electron. **23** (1987), 283.
[7] DELOUYA G., LEPRINCE P., MILLEOU H., Rev. Phys. Appl. **12** (1977), 969.
[8] IWASAKI CH., JITSUNO T., IEEE J. Quantum Elextron. **18** (1982), 432.
[9] GORSE C., CAPITELLI M., J. Appl. Phys. **62** (1987), 4072.

Received March 4, 1993